International Journal of Biology and Life Sciences
ISSN: 2957-9511 | Vol. 13, No. 3, 2026

Optimization and Evaluation of a Dendritic Cell-targeting Strategy based on Lipid Nanoparticle-mRNAVaccine

Lingyu Wang

YK Pao School, Shanghai, 201620, China

Abstract: Infectious diseases and cancer are major public health challenges facing the world today, posing a persistent threat to human health. Vaccines based on messenger RNA (mRNA) technology have demonstrated great potential in disease prevention and control due to their efficient delivery and immune activation capabilities. Although the use of lipid nanoparticles (LNPs) has significantly improved the intracellular delivery efficiency of mRNA, issues such as insufficient mRNA stability, poor targeting, limited expression levels, and cumulative liver toxicity still retain. This study proposes a dual optimization strategy for mRNA vaccines: by optimizing the untranslated region (UTR) sequence, introducing a 5' cap structure, and a segmented poly(A) tail at the 3' end, significantly enhancing mRNA stability and translation efficiency. And we innovatively employed mannose-modified polyethylene glycol (PEG)-coated lipid nanoparticles, leveraging mannose receptors on dendritic cells (DCs) to achieve active targeted delivery. This study effectively enhanced the targeting transfection efficiency of LNP/mRNA vaccines for dendritic cells, providing a new idea for the optimization strategy of LNP- based mRNA vaccines and having important application reference value for promoting tumor immunotherapy and the prevention and control of infectious diseases.

Keywords: mRNA Vaccine; DC Cell Targeting; Mannose Receptor; Cancer Prevention.

1. Introduction

Currently, mRNA vaccines have emerged as a promising approach for preventing and treating various diseases. However, mRNA is structurally unstable and exhibits low translation efficiency. Therefore, enhancing mRNA translation efficiency can be achieved by modifying different segments of mRNA and optimizing its design. The 5' cap is a modified nucleotide structure crucial for ensuring mRNA stability and efficient protein translation [1]. Adding a cap modification to the 5' end, particularly the m7G cap (m7GpppN), protects mRNA from nuclease attack, thereby enhancing mRNA stability and immunogenicity. This facilitates recognition of the mRNA by the translation initiation complex and improves translation efficiency [2]. Furthermore, in mRNA vaccines, open reading frame (ORF) design directly influences target antigen production. Optimizing ORF codons improves translation efficiency and prevents premature termination, while specific RNA modifications like pseudouridine enhance mRNA stability and accuracy [3]. The mRNA coding region determines the amino acid sequence of the protein, while the UTRs regulate its expression. Therefore, during mRNA vaccine design, selective modifications to the 5' UTR or 3' UTR can be made to target protein expression and immune response: modifying the 5' UTR enhances translation efficiency, while modifying the 3' UTR increases mRNA stability and prolongs protein expression duration, thereby improving the immunogenicity and efficacy of mRNA vaccines [4]. The polyadenylate tail is a post-transcriptional modification required for mRNA in eukaryotic cells, playing a crucial regulatory role in mRNA stability, export, and translation. By optimizing the length and sequence of the Poly(A) tail, it is possible to balance the trade-offs between mRNA stability and translation efficiency while maintaining both, thereby increasing the amount of expressed antigen and enhancing the immune response.

Furthermore, RNA is inherently unstable. Direct injection of naked mRNA molecules into cells or tissues triggers immune responses [5] and leads to degradation, posing significant challenges for intracellular mRNA vaccine delivery. In recent years, the two most common mRNA vaccine delivery systems have been lipid nanoparticles (LNPs) and polymeric nanoparticles [6]. LNPs are widely used in mRNA vaccine delivery systems due to their excellent biocompatibility, stability, and ability to protect mRNA from degradation [7]. The core structure of LNPs consists of ionizable cationic lipids, enabling the lipid nanoparticles to successfully encapsulate over 90% of the mRNA during the encapsulation process [8]. Concurrently, ionizable lipids partially explain the adjuvant properties of mRNA vaccines [9]. Distearoylphosphatidylcholine (DSPC), an auxiliary component in commercial lipid nanoparticles, reinforces LNP structure. It enhances lipid encapsulation efficiency while promoting cellular delivery of mRNA [10]. Polyethylene glycol (PEG)-modified LNPs feature a hydrophilic PEG coating on their surface, which helps improve biocompatibility and reduce toxicity [11]. PEG lipids constitute the least abundant component in LNP carriers but perform multiple critical functions, including maintaining final particle dispersion, mRNA encapsulation efficiency, and immunogenicity [12]. Cholesterol, meanwhile, makes a significant contribution to the membrane stability and structural integrity of LNPs [13]. This study structurally optimized the mRNA synthesis sequence and employed a composition of mannosylated lipid nanoparticle carriers, offering a viable solution for enhancing mRNA chain stability while addressing vaccine efficacy and safety concerns.

2. Results

2.1. Characterization of Novel Mannose-Coupled Man-LNP/mRNA

Following the design of mRNA sequence and chemical modifications, the complete mRNA molecule was obtained. To prepare LNP/mRNA liposomal nanoparticles required for subsequent experiments, this study employed a microfluidic device to mix and assemble a sodium citrate solution containing dissolved mRNA with a mixed lipid ethanol solution. Microfluidic devices precisely control two liquids via microfluidic chips, enhancing interactions between reaction fluids to enable rapid mutual reactions and expedite product generation. To preliminarily assess whether mannose modification adversely affects the structure of lipid nanoparticles, this study evaluated the impact by using either DMG-PEG2000 or DSPE-PEG2000-Mannose with other lipid components (DLin-MC3-DMA, DSPC, cholesterol) in a molar ratio of 1.5:50:10: 38.5 (PEG: DLin-MC3-DMA: DSPC: cholesterol) and a mass ratio of 20 (total lipids: mRNA) to synthesize conventional MC3 LNP/mRNA (Normal-LNP/mRNA or Nor-LNP/mRNA) and mannose-modified MC3 LNP/mRNA (Mannose-LNP/mRNA or Man-LNP/mRNA). Subsequently, both synthesized LNP/mRNA nanoparticles were characterized using gel electrophoresis retardation assays, particle size and surface potential measurements, and transmission electron microscopy to assess mRNA encapsulation efficiency, homogeneity, dispersion, morphology, and particle surface potential.

First, agarose gel electrophoresis was employed to assess lipid composition effects on mRNA assembly based on retention patterns. A 1% agarose gel was used, with naked mRNA serving as the control. As shown in Figure 1, comparison with the naked mRNA control revealed that both Man-LNP/mRNA and Nor-LNP/mRNA samples exhibited mRNA retention at the loading well's starting position on the gel. This indicates that both were restricted by the three-dimensional network structure of the electrophoresis gel, whereas naked mRNA migrated normally through the gel. At the level indicated by the naked mRNA electrophoresis band, no leaked mRNA bands were detected in the Man-LNP/mRNA or Nor-LNP/mRNA loading groups. This demonstrates that both Man-LNP/mRNA and Nor-LNP/mRNA effectively encapsulate mRNA completely within the solution. This demonstrates that Mannose-LNP/mRNA exhibits comparable encapsulation efficiency to Nor-LNP/mRNA following mannose modification. The presence of mannose components in Mannose-LNP/mRNA does not interfere with the LNP's inherent mRNA assembly capability.

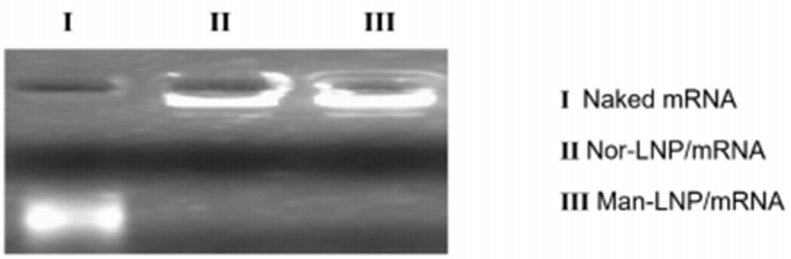

Figure 1. Agarose gel electrophoresis results for different LNP-mRNA formulations

A 1% agarose gel was used to visualize the electrophoresis patterns of different components, with the top of the figure indicating the electrophoresis starting position. Naked mRNA (I), Conventional LNP/mRNA (II), Mannose-modified LNP/mRNA (III). Electrophoresed at 100 V for 20 minutes.

Pipette an appropriate volume of ultrafiltrated LNP/mRNA particle solutions (containing approximately 1 μg mRNA molecules) and dilute with 1 mL RNA-free water. Transfer the diluted particle solutions to the nanoparticle zeta potential analyzer cell for simultaneous measurement of particle size distribution and surface potential. The nanoparticle size analyzer is an experimental instrument based on dynamic light scattering and electrophoretic light scattering technology, used for precise determination of nanoparticle size distribution and zeta potential. It is widely applied in various research areas, including LNP drug carrier optimization, nanomaterial stability assessment, and biomolecular characterization analysis.

The particle size distribution within the 0–1000 nm range was statistically plotted, yielding the results shown in Figure 2 (right). Both conventional Nor-LNP/mRNA and mannose-modified Man-LNP/mRNA particles exhibited nanoscale dimensions, qualifying them as lipid nanoparticles. The average particle size of both LNP/mRNA lipid nanoparticles was approximately 230 nm. Additionally, the particle size distribution of the improved Man-LNP/mRNA was observed to be more concentrated compared to Nor-LNP/mRNA, indicating superior uniformity.

Surface potential measurements of different LNP/mRNA particle solutions are shown in Figure 4.2 [Left]. Both conventional Nor-LNP/mRNA and mannosyl-modified Man-LNP/mRNA particles carry positive charges on their surfaces. Compared to conventional Nor-LNP/mRNA, mannosyl-modified Man-LNP/mRNA exhibits a higher positive potential. Based on the above results, it can be inferred that compared to conventional Nor-LNP/mRNA, mannosyl-modified Man-LNP/mRNA exhibits two advantages: 1) Since mRNA sequences inherently carry a negative charge, a stronger positive charge on the mannosyl-modified mRNA lipid nanoparticles (Man-LNP/mRNA) implies enhanced assembly capability with the negatively charged mRNA; 2) Since target cell membranes carry a negative charge, we predict that the improved Man-LNP/mRNA will be more readily internalized by cell membranes, thereby enhancing the transfection efficiency of mRNA vaccine particles within cells.

The green legend represents conventional LNP/mRNA particles without mannose modification, while the red legend indicates mannose-modified Man-LNP/mRNA particles. The left panel indicates that the mRNA vaccine nanoparticles exhibit a higher positive zeta potential after mannose modification. The right panel shows that the modified nanoparticles possess a more narrowed particle size distribution. Both types of LNP/mRNA particles have an

average diameter of approximately 230 nm.

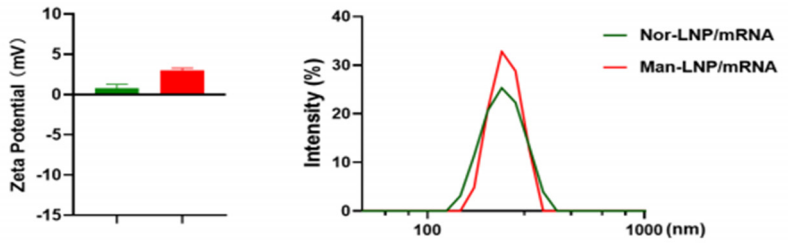

Figure 2. Surface potential and particle size distribution of different LNP/mRNA formulations

Subsequently, transmission electron microscopy (TEM) was employed to observe the true morphology of nanoparticles in solution. Droplets of different LNP/mRNA particle solutions were applied to copper grids for sample preparation and imaging. TEM utilizes the elastic/inelastic scattering of high-energy electron beams with the sample, combined with sub-angstrom resolution imaging and multimodal analysis, to achieve detailed structural characterization of nanoparticles. The imaging results are shown in Figure 3. The images reveal that the particles are relatively independent, without agglomeration, uniformly dispersed, and exhibit regular shapes. This indicates excellent nanoparticle morphology, with no aggregation occurring in solution that could interfere with the nanoparticle structure. By comparing the nanoparticle morphology of the mannose-modified mRNA vaccine with that of the standard mRNA vaccine, it can be further confirmed that mannose modification does not interfere with the excellent properties of the LNP/mRNA nanoparticle delivery system.

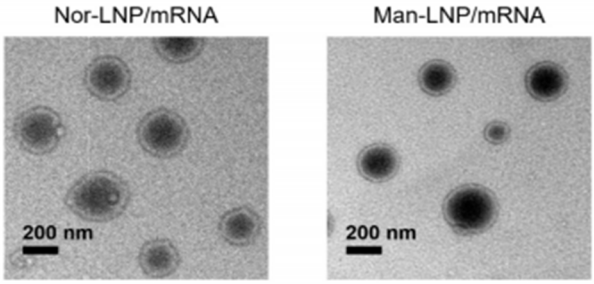

Figure 3. Transmission electron microscopy images of different LNP/mRNA nanoparticles.

The left image shows the morphology of Nor-LNP/mRNA nanoparticles, while the right image displays the morphology of Man-LNP/mRNA nanoparticles. Scale bar: 200 nm.

2.2. Man-LNP/mRNA Enhances Expression Levels in DC Cells

To quantify the transfection efficiency of different LNP/mRNA nanoparticles in dendritic cells, we selected the dendritic cell line DC 2.4 and used mRNA encoding enhanced green fluorescent protein (EGFP) ($mRNA^{EGFP}$) as the model mRNA. $mRNA^{EGFP}$ was assembled with mixed lipid components into conventional Nor-LNP/mRNA and mannose-modified Man-LNP/mRNA, which were then used to transfect DC 2.4 cells. Cells were harvested 24 hours post-transfection, and EGFP expression levels were detected using flow cytometry. This transfection experiment included distinct control groups: the PBS group served as a baseline for experimental measurements; the $mRNA^{EGFP}$-only group assessed whether naked mRNA could be cellularly internalized and expressed; and the Mock-LNP group (unloaded lipid nanoparticles without $mRNA^{EGFP}$) excluded effects of LNP components on cells and fluorescence detection.

Direct flow cytometer data for different transfection groups are shown in Figure 4 (Left). The left panel displays the fluorescence peak plot generated by the flow cytometer, where peak shift indicates fluorescence signal intensity. The black dashed line delineates the EGFP-negative/positive threshold, with the left side representing negative and the right side positive. The right panel presents statistical results for the proportion of EGFP-positive cells. Neither the $mRNA^{EGFP}$-only group nor the Mock-LNP group showed differences compared to the PBS control group, indicating that $mRNA^{EGFP}$ alone cannot enter cells and express. Furthermore, the lipid components represented by Mock-LNP do not affect cells or fluorescence detection. For the key experimental groups Nor-LNP/mRNA and Man-LNP/mRNA, both LNP/mRNA transfections produced distinct fluorescence signal shifts in DC 2.4 cells. Although the fluorescence distribution range showed no significant difference, the mannosylation modification of Man-LNP/mRNA markedly reduced the peak area of the EGFP-negative cell population.

Statistical analysis of EGFP-positive cell proportions across three replicate experiments and different transfection groups yielded the results presented in Figure 4 (right). As shown in Figure 4 (right), EGFP-positive cell proportions in the PBS control, $mRNA^{EGFP}$ alone, and Mock-LNP groups were all near 0%, indicating no false-positive signal interference. The EGFP-positive proportion in the Nor-LNP/mRNA-EGFP transfection group was approximately 59%, while that in the Man-LNP/mRNA-EGFP transfection group reached about 75%, representing a significant improvement compared to the Nor-LNP/mRNA group. This demonstrates that the modified mRNA vaccine exhibits enhanced cellular targeting, transfection efficiency, and protein expression success rates. This may be a beneficial outcome of the synergistic effect between the positive charge of the Man-LNP/mRNA nanoparticles themselves and the mannose modification used for DC cell targeting. Based on this, it can be boldly predicted that using such carriers to deliver pathogen antigen mRNA could enable more cells to express antigen proteins, thereby inducing a stronger and more intense immune response. Furthermore, the improved transfection efficiency indicates an increased uptake rate of LNP/mRNA nanoparticles by cells, which indirectly mitigates toxicity accumulation issues.

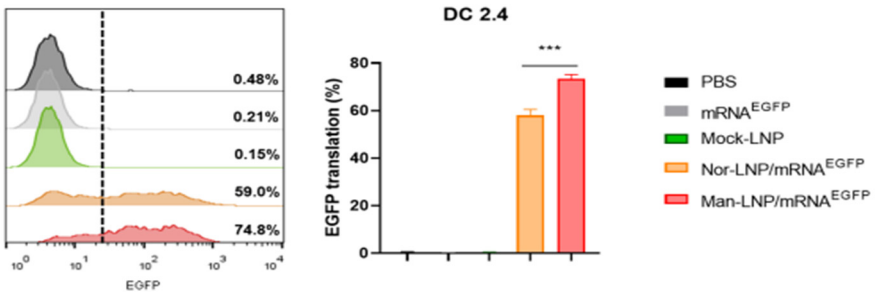

Figure 4. Statistical results of transfection efficiency for different LNP/mRNA^{EGFP} formulations in DC 2.4 cells

The proportion of EGFP-positive cells in DC 2.4 cells was detected by flow cytometry 24 hours after transfection with PBS, mRNA^{EGFP}, Mock-LNP, Nor-LNP/mRNA^{EGFP}, or Man-LNP/mRNA^{EGFP}. The left panel shows the fluorescence distribution histogram from flow cytometry, where the shift of the peak represents the intensity of the fluorescence signal. The black dashed line delineates the threshold separating EGFP-negative from EGFP-positive cells, with the left side indicating negative and the right side indicating positive. The right panel shows statistical results for the proportion of EGFP-positive cells. n = 3. Significant differences between groups were calculated using the t-test method. *** $p < 0.001$.

2.3. Man-LNP/mRNA Further Stimulates BMDC Maturation

After confirming the enhanced delivery efficiency of the improved Man-LNP/mRNA system to dendritic cell lines using mRNAEGFP, mRNA encoding the model antigen protein OVA (mRNAOVA) was employed to investigate the maturation levels and antigen presentation induction efficiency of both LNP/mRNA nanoparticles in primary dendritic cells. Primary bone marrow-derived dendritic cells (BMDCs) were isolated and cultured directly from mouse bone marrow, preserving the natural characteristics of in vivo DCs (such as antigen uptake, migratory capacity, and surface molecule expression), thereby making experimental results more closely resemble real biological processes. DC maturation is crucial for activating downstream T cells and represents a key step in the immune response. CD86 and CD80 serve as key markers for distinguishing the maturity status of dendritic cells (CD11c+). Fluorescently labeled antibodies were used to incubate and mark the transfected BMDCs. During flow cytometry analysis, these fluorescently conjugated antibodies bind to the surface proteins of CD86 and CD80, emitting fluorescence upon excitation, which is then detected by the flow cytometer. By observing the fluorescence intensity across experimental groups, the efficiency of the two LNP/mRNAOVA formulations in inducing BMDC maturation was analyzed.

Using the same experimental groups and controls as the previous transfection experiment (as shown in Figure 5), statistical analysis was performed on the proportion of CD86 and CD80 double-positive cells within CD11c-positive cells (representing DCs). The results revealed that the maturation rates of BMDCs in the PBS control group, the mRNA-EGFP-only treatment group, and the Mock-LNP treatment group did not exceed 20%, indicating that these materials lacked stimulatory effects. Compared to Nor-LNP/mRNAOVA, Man-LNP/mRNAOVA significantly enhanced the upregulation of CD80 and CD86 expression levels in BMDCs. This indicates that the improved Man-LNP/mRNA vaccine can further stimulate DC maturation and promote the formation of specific immunity. Since immunogenicity is a crucial factor in DC maturation induction, these results may also suggest that the improved Man-LNP/mRNA vaccine possesses higher immunogenicity, potentially enhancing antigen presentation and signal transduction.

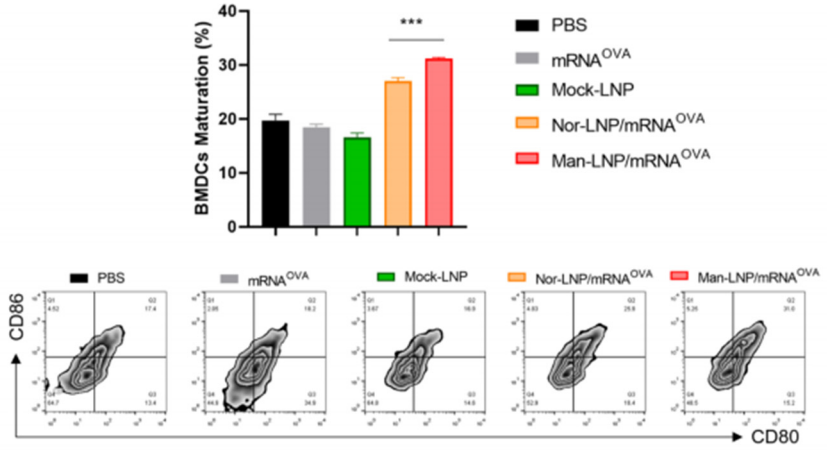

Figure 5. Statistical chart of the maturation induction rate by different LNP/mRNAOVA in BMDCs and representative flow cytometry images.

Flow cytometric analysis of CD80+CD86+ cells in CD11c+ BMDCs 24 hours after transfection with PBS, mRNA^{EGFP}, Mock-LNP, Nor-LNP/mRNA^{EGFP}, or Man-LNP/mRNA^{EGFP}. Mock-LNP represents empty LNP. The upper panel shows the proportion of CD80+CD86+ cells within the CD11c+ cell population. The lower panel displays representative flow cytometric images. n = 3. Significant differences between groups were calculated using the t-test

method. *** $p < 0.001$.

2.4. Man-LNP/mRNA Vaccines Further Enhance Antigen Presentation Efficiency in BMDCs

Subsequently, this study continued using mRNA-OVA to explore the antigen presentation efficiency induced by BMDCs following treatment with two LNP/mRNA formulations. OVA, as a model antigen, is T-cell-dependent and can activate specific T-cell responses by being presented by DCs via MHC molecules on the cell surface. Statistical analysis was performed on the proportion of CD11c-positive cells (representing DCs) expressing OVA epitope peptides complexed with MHC class I molecules (SIINFEKL-H2Kb). Results are shown in Figure 6. In the PBS group, the mRNAOVA-only group, and the Mock-LNP group, the SIINFEKL-H2Kb-positive proportion was below 5%, with minor false-positive signal interference. Compared to the PBS group, the mRNAOVA-only treatment group showed a trend toward approximately a 2% increase in positive signals, but no significant difference was observed. Representative flow cytometry data from Nor-LNP/mRNAOVA and Man-LNP/mRNAOVA-treated BMDCs showed a distinct shift toward positive cell populations, as indicated by the black boxes in the figure. Comparing Nor-LNP/mRNAOVA with Man-LNP/mRNAOVA reveals that mannosyl-modified Man-LNP/mRNA induces a higher proportion of specific antigen presentation. This indicates that Man-LNP/mRNAOVA is taken up by a greater number of BMDCs, thereby presenting the encoded antigen on the cell surface, demonstrating the DC-targeted delivery efficacy of Man-LNP/mRNAOVA.

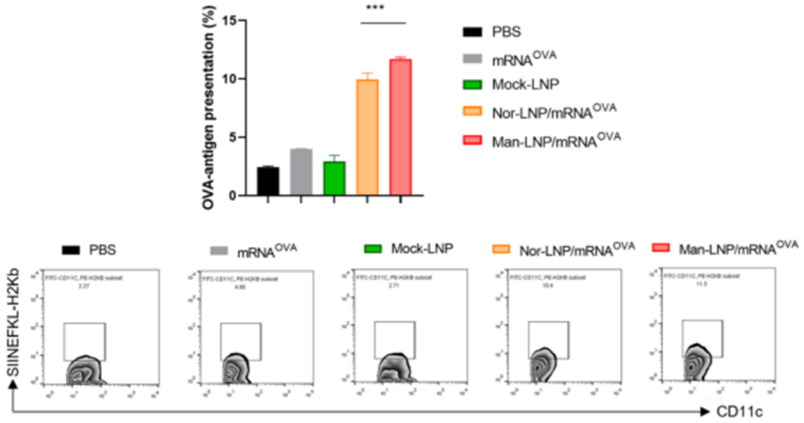

Figure 6. Statistical chart showing the proportion of antigen presentation promoted by different LNP/mRNAOVA in BMDCs and representative flow cytometry images.

Flow cytometric analysis of SIINFEKL-H2Kb-positive cells in CD11c-positive BMDCs 24 hours after transfection with PBS, mRNAEGFP, Mock-LNP, Nor-LNP/mRNAEGFP, or Man-LNP/mRNAEGFP. Mock-LNP represents empty LNP. The upper panel shows the proportion of SIINFEKL-H2Kb-positive cells within the CD11c-positive cell population. The lower panel displays representative flow cytometric images, with the black box indicating the target cell population. n = 3. Significant differences between groups were calculated using the t-test method. *** $p < 0.001$.

2.5. Man-LNP/mRNA Vaccine Significantly Inhibits Tumor Growth

After confirming that Man-LNP/mRNA enhances the maturation of BMDCs and boosts antigen presentation, a mouse tumor prevention experiment was carefully designed to further validate the improved efficacy of the Man-LNP/mRNA vaccine in preventing tumor growth at the in vivo level. B16-OVA cells are genetically modified mouse melanoma cells expressing OVA protein, enabling OVA to serve as a unique antigen for B16 cells. This animal prevention study utilized B16-OVA cells to establish a mouse melanoma tumor model. As shown in the experimental schedule in Figure 7(upper), healthy female C57/BL mice received intradermal injections (i.d.) on Day 0 and Day 7 with saline, naked mRNA-OVA, Nor-LNP/mRNA-OVA, or Man-LNP/mRNA-OVA, respectively. On day 14, B16-OVA tumor cells were injected subcutaneously (s.c.) into the opposite side of the mouse back. Tumor size on the mouse back was measured using calipers every two to three days. Tumor growth data and mouse survival data were collected for statistical analysis.

Tumor growth volume data, as shown in Figure 7(middle), indicate that tumors in mice immunized with saline (blank), naked mRNAOVA, Nor-LNP/mRNAOVA, or Man-LNP/mRNAOVA exhibited no significant growth during the initial 10 days. After 10 days, tumors in mice immunized with blank and naked mRNAOVA began rapid growth. Tumors in the blank group first exceeded 1500 mm^3 on day 27, demonstrating strong proliferative capacity. This excluded issues with experimental mice or tumor cell lines, confirming no interference with tumor growth. In both LNP/mRNAOVA groups, tumor growth was significantly suppressed. Compared to the Nor-LNP/mRNAOVA immunized group, the Man-LNP/mRNAOVA immunized group exhibited the slowest tumor growth. By day 27, the average tumor volume in the five mice of the Man-LNP/mRNAOVA immunized group was only around 50 mm^3, while that in the five mice of the Nor-LNP/mRNAOVA immunized group was approximately 180 mm^3, representing a significant difference.

The mouse survival curve data are shown in Figure 7 (bottom). Mice immunized with saline (blank) or naked mRNAOVA rapidly died within 24–33 days, with a survival rate of 0%. In contrast, the survival time of mice in the Nor-LNP/mRNAOVA or Man-LNP/mRNAOVA immunized groups was significantly prolonged. The first mouse death in the Nor-LNP/mRNAOVA group occurred on day 36, while the first death in the Man-LNP/mRNAOVA group occurred on day 48. Within 60 days, mortality rates in both LNP/mRNAOVA and Man-LNP/mRNAOVA immunized groups gradually increased. However, ultimately, one mouse

in the Nor-LNP/mRNAOVA group survived completely, yielding a 20% survival rate, while two mice in the Man-LNP/mRNAOVA group survived completely, achieving a 40% survival rate—a significant advantage. Thus, the mannosyl-modified mouse-derived nanoparticles increased survival rates from 20% to 40% compared to the normal vaccination group, indicating that Man-LNP/mRNA vaccines exhibit enhanced overall preventive efficacy following mannosyl-targeted modification.

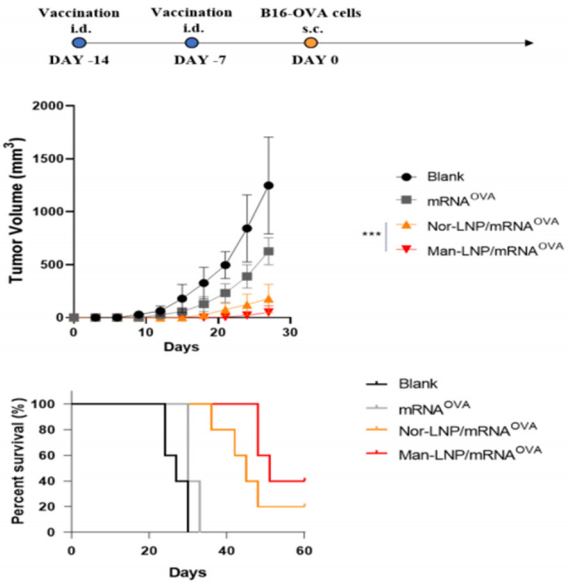

Figure 7. Growth of B16-OVA tumors in mice immunized with different LNP/mRNAOVA formulations and survival curves for mice in each experimental group.

The upper panel shows the long-term experimental schedule for the animal studies. On Days 0 and 7 of the experiment, healthy female C57/BL mice received intradermal injections (i.d.) of water, naked mRNAOVA, Nor-LNP/mRNAOVA, or Man-LNP/mRNAOVA on their backs, respectively. Each mouse received 10 μg of mRNAOVA per immunization. The four groups (n=5 mice per group) were identified by ear tags. On day 14, 1×10^6 B16-OVA tumor cells were injected subcutaneously (s.c.) into the opposite side of the back. Tumor size on the back was measured every 2–3 days using a caliper. Tumor volume (mm^3) = length × width × height/2. Mice were considered deceased when tumor volume exceeded 1500 mm^3. The middle panel shows collected tumor growth data, and the bottom panel shows mouse survival data. i.d. intradermal injection, s.c. subcutaneous injection. n = 5. Significant differences were calculated using the t-test method. *** $p < 0.001$.

3. Summary

This study addresses recent research trends and improvement opportunities in mRNA vaccine stability and targeted delivery. We propose and validate a dual-optimization approach based on LNPs to comprehensively enhance mRNA vaccine transfection efficiency and cell-specific delivery capabilities. Through optimizing untranslated regions (UTRs), this study selected the NASAR combination, introduced a segmented poly(A) tail structure, employed N1-methyl-pseudouridine (m1Ψ) for nucleoside modification, and performed 5'-capping. These modifications enhance mRNA sequence stability and translation efficiency while reducing the mRNA molecule's inherent immunogenicity. This allows target cells to focus on processing the encoded antigen protein for presentation. capping treatment to enhance mRNA sequence stability and translation efficiency. This approach also reduces the inherent immunogenicity of the mRNA molecule, enabling target cells to focus more on processing and presenting the encoded antigen protein. By incorporating mannose-modified PEG lipids (DSPE-PEG2000-Mannose) into the LNP formulation, a Man-LNP vector with targeted affinity for mannose receptors on DC cell membranes was constructed. The novel Man-LNP/mRNA vaccine maintains excellent nanostructure morphology and dispersibility while exhibiting higher surface positive charge. Compared to Nor-LNP, it demonstrates superior transfection efficiency in DCs and induces more pronounced cellular maturation and specific antigen presentation in BMDCs. Subsequent immunization with Man-LNP/mRNA effectively suppressed tumor growth and extended survival in tumor-bearing mice, increasing survival rates to 40%. This work provides a viable approach for optimizing LNP-delivered mRNA vaccines, offering significant implications for tumor immunotherapy and infectious disease prevention.

References

[1] Buschmann, M.D., et al., Nanomaterial Delivery Systems for mRNA Vaccines. Vaccines (Basel), 2021. 9(1).

[2] Patil, S., et al., The Development of Functional Non-Viral Vectors for Gene Delivery. Int J Mol Sci, 2019. 20(21).

[3] Lou, G., et al., Delivery of self-amplifying mRNA vaccines by cationic lipid nanoparticles: The impact of cationic lipid selection. J Control Release, 2020. 325: p. 370-379.

[4] Son, S. and K. Lee, Development of mRNA Vaccines/ Therapeutics and Their Delivery System. Mol Cells, 2023. 46 (1): p. 41-47.

[5] Kashem, S.W., M. Haniffa, and D.H. Kaplan, Antigen-Presenting Cells in the Skin. Annu Rev Immunol, 2017. 35: p. 469-499.

[6] Dunbar, C.E., et al., Gene therapy comes of age. Science, 2018. 359(6372).

[7] Gilbertson, S., et al., Changes in mRNA abundance drive shuttling of RNA binding proteins, linking cytoplasmic RNA degradation to transcription. Elife, 2018. 7.

[8] Alameh, M.G., et al., Lipid nanoparticles enhance the efficacy of mRNA and protein subunit vaccines by inducing robust T follicular helper cell and humoral responses. Immunity, 2021. 54(12): p. 2877-2892 e7.

[9] Kulkarni, J.A., et al., Design of lipid nanoparticles for in vitro and in vivo delivery of plasmid DNA. Nanomedicine, 2017. 13(4): p. 1377-1387.

[10] Suzuki, T., et al., PEG shedding-rate-dependent blood clearance of PEGylated lipid nanoparticles in mice: Faster PEG shedding attenuates anti-PEG IgM production. Int J Pharm, 2020. 588: p. 119792.

[11] Kranz, L.M., et al., Systemic RNA delivery to dendritic cells exploits antiviral defence for cancer immunotherapy. Nature, 2016. 534(7607): p. 396-401.

[12] Gao, H., et al., Comparative binding and uptake of liposomes decorated with mannose oligosaccharides by cells expressing the mannose receptor or DC-SIGN. Carbohydr Res, 2020. 487: p. 107877.

[13] Jamous, Y.F. and D.A. Alhomoud, The Safety and Effectiveness of mRNA Vaccines Against SARS-CoV-2. Cureus, 2023. 15(9): p. e45602.